



Since January 2020 Elsevier has created a COVID-19 resource centre with free information in English and Mandarin on the novel coronavirus COVID-19. The COVID-19 resource centre is hosted on Elsevier Connect, the company's public news and information website.

Elsevier hereby grants permission to make all its COVID-19-related research that is available on the COVID-19 resource centre - including this research content - immediately available in PubMed Central and other publicly funded repositories, such as the WHO COVID database with rights for unrestricted research re-use and analyses in any form or by any means with acknowledgement of the original source. These permissions are granted for free by Elsevier for as long as the COVID-19 resource centre remains active.



# XBB.1.5 Kraken cracked: Gibbs energies of binding and biosynthesis of the XBB.1.5 variant of SARS-CoV-2

Marko E. Popovic

School of Life Sciences, Technical University of Munich, 85354 Freising, Germany

## ARTICLE INFO

### Keywords:

Omicron variant  
Infectivity  
Pathogenicity  
Biothermodynamics  
COVID-19  
Viral evolution

## ABSTRACT

The SARS-CoV-2 Hydra with many heads (variants) has been causing the COVID-19 pandemic for 3 years. The appearance of every new head (SARS-CoV-2 variant) causes a new pandemic wave. The last in the series is the XBB.1.5 “Kraken” variant. In the general public (social media) and in the scientific community (scientific journals), during the last several weeks since the variant has appeared, the question was raised of whether the infectivity of the new variant will be greater. This article attempts to provide the answer. Analysis of thermodynamic driving forces of binding and biosynthesis leads to the conclusion that infectivity of the XBB.1.5 variant could be increased to a certain extent. The pathogenicity of the XBB.1.5 variant seems to be unchanged compared to the other Omicron variants.

## 1. Introduction

SARS-CoV-2 is a real creature, which associates of the mythical creature Hydra. In the myth, Hydra is a monster with multiple heads. When one of Hydra’s heads is cut off, two more appear. SARS-CoV-2 virus has appeared in the human population in 2019, as the Hu-1 wild type and caused the first wave of the COVID-19 pandemic. SARS-CoV-2 has jumped the inter-species barrier (Popovic, 2022e). By cutting off the head of Hu-1, new variants appeared through time, which were labeled using the Greek alphabet. During the last 3 years, we used up the entire Greek alphabet on various strains of SARS-CoV-2. The last in the series is the XBB.1.5 variant, known as the Kraken. Newer variants have caused pandemic waves and suppressed the old variants. The appearance of new variants and new pandemic waves have caused fear in the population and governments of all countries. Every time a new strain appears, the question is raised of whether it will be more infective and pathogenic than the previous ones, as well as will it be able to avoid immune response (Stacy, 2023; Browne, 2023). The situation is similar with the Omicron XBB.1.5 variant.

With appearance of the COVID-19 pandemic, a great effort was made by scientists to follow the time evolution of SARS-CoV-2, as well as to develop antiviral medicines and vaccines (Tang et al., 2020; Phan, 2020; Singh and Yi, 2021). The XBB.1.5 variant has been spreading fast during the last weeks in America, Europe and Far East. In the literature, dissociation equilibrium constants were reported for the variants that are in circulation (Yue et al., 2023). The study found that the

transmissibility of XBB.1.5 is increased, due to the contribution of strong ACE2 binding and immune evasion (Yue et al., 2023).

The binding of the spike glycoprotein to the ACE2 receptor represents a chemical reaction similar to protein-ligand interactions (Du et al., 2016; Popovic and Popovic, 2022). This is why the antigen-receptor binding rate depends on the driving force of the reaction, according to the phenomenological equation (Popovic, 2022a; 2022b; Demirel, 2014; Balmer, 2010). The driving force for the reaction of antigen-receptor binding is Gibbs energy of binding (Popovic, 2022c; 2022d; Gale, 2022, 2020, 2019, 2018). Gibbs energies of binding have been reported for all SARS-CoV-2 variants (Popovic and Popovic, 2022; Popovic, 2022a; 2022b; 2022c; 2022d; 2022e; 2022g; 2022h; 2022i). The great entry rate of viruses into host cells indicates the level of infectivity. Infectivity also depends on concentration of virus particles in the air (Guallar et al., 2020; Van Damme et al., 2021; Spinelli et al., 2021). The concentration of virus particles in the air is greater in closed spaces. This is why infection is more likely in closed spaces than in open spaces. The concentration of virus particles in space also depends on production and excretion of particles by the infected person. This is why infectivity cannot be estimated solely using binding affinity, nor even Gibbs energy of binding. Infectivity also depends on the rate of biosynthesis of virus components, and self-assembly of virus components into new virions and their excretion. Fast multiplication of the virus followed by excretion leads to increase in virus concentration in closed spaces and greater infectivity.

The multiplication rate of the virus also influences pathogenicity. A

E-mail addresses: [marko.popovic@tum.de](mailto:marko.popovic@tum.de), [marko.popovic.td@gmail.com](mailto:marko.popovic.td@gmail.com).

<https://doi.org/10.1016/j.micres.2023.127337>

Received 22 January 2023; Received in revised form 12 February 2023; Accepted 14 February 2023

Available online 15 February 2023

0944-5013/© 2023 Elsevier GmbH. All rights reserved.

greater rate of virus biosynthesis (multiplication, which includes replication, transcription, translation, self-assembly and maturation) leads to greater damage to cells and tissues, which corresponds to greater pathogenicity.

Since all SARS-CoV-2 variants have been chemically and thermodynamically characterized, it is possible to follow the time evolution of thermodynamic properties of the virus, infectivity and pathogenicity. Thermodynamic analysis shows that the reported trend in SARS-CoV-2 evolution towards more negative Gibbs energy of binding and tendency towards mildly negative Gibbs energy of biosynthesis (Popovic, 2022i). These changes in biothermodynamic properties are a consequence of more frequent acquisition of mutations by SARS-CoV-2. Replacement of one nucleotide by another results in change in elemental composition (empirical formula) of the newly appeared variant (Popovic, 2022f; 2022i). Changes in empirical formula result in changes in Gibbs energy of the new variant (Popovic, 2022f; 2022i). Empirical formulas of SARS-CoV-2 have been reported in the literature (Şimşek et al., 2021; Degueldre, 2021).

Elemental composition of virus particles can be determined using the atom counting method (Popovic, 2022j) or by experiment (Degueldre, 20210). Atom counting method determines elemental composition of viruses based on their genetic and protein sequences, and morphology (Popovic, 2022j). It is highly accurate and should in theory be able to determine the structure within one atom accuracy (Popovic, 2022j). The results from the atom counting method were found to be in very good agreement with experimental results (Popovic, 2022j). Experimental methods for elemental analysis, such as ICP-MS, are among the most accurate chemical analysis methods available (Degueldre, 2021). More information about the accuracy of such methods and their applicability to viruses has been discussed by Degueldre (2021). Viruses consist of many copies of proteins, which are encoded by the viral nucleic acid (Şimşek et al., 2021). Changes in viral nucleic acid lead to changes in the protein sequences. The changes in protein sequences are amplified by the large number of protein copies in virus particles (Popovic, 2022j). Thus, the different protein sequences are reflected in different elemental composition of the virus particle and different relative masses (Popovic, 2022j).

Mutations can appear in the part of the viral genome that encodes the spike glycoprotein or the rest of the genome. Mutations of the part that encodes the spike glycoprotein lead to changes in binding affinity, binding constant, dissociation constant, as well as enthalpy, entropy and Gibbs energy of binding (Popovic, 2022g; 2022i). Mutations that appear on the rest of the viral nucleic acids, together with mutations on the spike encoding segments, lead to changes in Gibbs energy of biosynthesis of the virus (Popovic, 2022f; 2022i). Changes in Gibbs energy, according to the phenomenological equations, lead to changes in kinetics (rate of antigen-receptor binding and rate of virus multiplication). It is not enough to use only the binding affinity ( $K_d$ ) for estimating virus-host interactions at the membrane and in the cytoplasm. However, the virus strain characterized with a greater number of mutations, greater change in elemental composition, and more negative Gibbs energies of binding and biosynthesis exhibits greater infectivity. But, the spreading of the disease does not depend only on virus infectivity, but also on the immunization of the population, therapy and application of epidemiological measures. Spreading and pathogenesis of SARS-CoV-2 has been discussed from biothermodynamic perspective (Lucia et al., 2021, 2020a; 2022b; Kaniadakis et al., 2020; Nadi and Özilgen, 2021; Özilgen and Yilmaz, 2021; Yilmaz et al., 2020; Head et al., 2022).

The goal of this paper is to perform a chemical and thermodynamic characterization of the XBB.1.5 Kraken variant of SARS-CoV-2, to estimate the risk that the new variant could represent for the population. This will be achieved by applying the atom counting method for determining the empirical formula of the variant (Popovic, 2022j). Based on the elemental composition, growth reactions will be formulated, based on which thermodynamic properties of formation and biosynthesis will be calculated, using predictive biothermodynamic

models. Moreover, Gibbs energy of SGP-ACE2 binding will be calculated for the XBB.1.5 variant. The calculated thermodynamic properties will be applied for thermodynamic analysis and implications on infectivity and pathogenicity of the XBB.1.5 variant.

## 2. Methods

### 2.1. Data sources

Genetic sequences of isolates of the XBB.1.5 “Kraken” variant of SARS-CoV-2 were taken from GISAID, the global data science initiative (Khare et al., 2021; Elbe and Buckland-Merrett, 2017; Shu and McCauley, 2017; GISAID, 2023). The genetic sequence of the XBB.1.5 isolate from Chile can be found under the accession code EPI\_ISL\_16370682 and is labeled hCoV-19/Chile/RM-137638/2022. It was isolated on December 18, 2022, in Las Condes, in the Region Metropolitana de Santiago. The genetic sequence of the XBB.1.5 isolate from India can be found under the accession code EPI\_ISL\_16378695 and is labeled hCoV-19/India/TG-CDFD-MMG-504/2022. It was isolated on December 31, 2022, in Hyderabad, in the state of Telangana. The genetic sequence of the XBB.1.5 isolate from Netherlands can be found under the accession code EPI\_ISL\_16446510 and is labeled hCoV-19/Netherlands/OV-RIVM-122353/2022. It was isolated on December 15, 2022, in the province of Overijssel. The genetic sequence of the XBB.1.5 isolate from Scotland can be found under the accession code EPI\_ISL\_16457174 and is labeled hCoV-19/Scotland/QEUH-3266AE29/2022. It was isolated on December 20, 2022, by a lab from Glasgow. The genetic sequence of the XBB.1.5 isolate from USA can be found under the accession code EPI\_ISL\_16454254 and is labeled hCoV-19/USA/TX-HMH-MCoV-121261/2022. It was isolated on December 27, 2022, in Houston, Texas. Therefore, the findings of this study are based on metadata associated with 5 sequences available on GISAID up to January 17, 2023, and accessible at <https://doi.org/10.55876/gis8.230117yo> More information about the genetic sequences can be found in the Supplementary Material.

The sequence of the nucleocapsid phosphoprotein of SARS-CoV-2 was obtained from the NCBI database (Sayers et al., 2022; National Center for Biotechnology Information, 2022), under the accession ID: UKQ14424.1. The number of copies of the nucleocapsid phosphoprotein in virus particle was taken from (Neuman and Buchmeier, 2016; Neuman et al., 2011; Neuman et al., 2006).

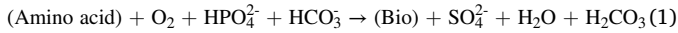
The dissociation equilibrium constants,  $K_d$ , of the BQ.1.1, XBB/XBB.1, XBB.1.5 and BA.2.75 variants of SARS-CoV-2 were taken from (Yue et al., 2023). They were measured at 25 °C, using surface plasmon resonance (Yue et al., 2023).

### 2.2. Empirical formulas and biosynthesis reactions

The genetic and protein sequences were used to find empirical formulas of nucleocapsids of the BA.5.2 and BF.7 variants of SARS-CoV-2. This was done using the atom counting method (Popovic, 2022j). The atom counting method is implemented using a computer program (Popovic, 2022j). The input are genetic and protein sequences of the virus of interest, as well as the number of copies of proteins in the virus particle and the virus particle size (Popovic, 2022j). The program goes along the nucleic acid and protein sequences and adds atoms coming from each residue in the sequence, to find the number of atoms contributed by that macromolecule to the virus particle (Popovic, 2022j). The contributions of viral proteins are multiplied by their copy numbers, since proteins are present in multiple copies in virus particles (Popovic, 2022j). The output of the program is elemental composition of virus particles, in the form of empirical formulas, and molar masses of virus particles (Popovic, 2022j). The advantage of the atom counting method is that it can provide the empirical formulas of virus particles, based on widely available data on genetic and protein sequences (Popovic, 2022j). The atom counting method was shown to give results

in good agreement with experimental results (Popovic, 2022j).

The empirical formulas of virus particles were used to construct biosynthesis reactions, summarizing conversion of nutrients into new live matter (von Stockar, 2013a, 2013b; Battley, 1998). The biosynthesis reaction for virus particles has the general form.



where (Bio) represents new live matter, described by an empirical formula given by the atom counting method (Popovic, 2022b; 2022c; 2022f). (Amino acid) represents a mixture of amino acids with the empirical formula  $\text{CH}_{1.798}\text{O}_{0.4831}\text{N}_{0.2247}\text{S}_{0.022472}$  (expressed per mole of carbon), representing the source of energy, carbon, nitrogen and sulfur (Popovic, 2022b; 2022c; 2022f).  $\text{O}_2$  is the electron acceptor (Popovic, 2022b; 2022c; 2022f).  $\text{HPO}_4^{2-}$  is the source of phosphorus (Popovic, 2022b; 2022c; 2022f).  $\text{HCO}_3^-$  is a part of the bicarbonate buffer that takes excess  $\text{H}^+$  ions that are generated during biosynthesis (Popovic, 2022b; 2022c; 2022f).  $\text{SO}_4^{2-}$  is an additional metabolic product that takes excess sulfur atoms (Popovic, 2022b; 2022c; 2022f).  $\text{H}_2\text{CO}_3$  takes the oxidized carbon atoms and is also a part of the bicarbonate buffer (Popovic, 2022b; 2022c; 2022f).

### 2.3. Thermodynamic properties of live matter and biosynthesis

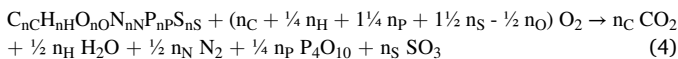
Empirical formulas of virus nucleocapsids were used to find standard thermodynamic properties of their live matter, using predictive bi-thermodynamic models: the Patel-Erickson and Battley equations (Patel and Erickson 1981; Battley 1999, 1998, 1992; Battley and Stone 2000). The Patel-Erickson equation was used to find enthalpy of live matter, based on its elemental composition. The Patel-Erickson equation gives standard enthalpy of combustion,  $\Delta_c H^\circ$ , of live matter

$$\Delta_c H^\circ(\text{bio}) = -111.14 \frac{\text{kJ}}{\text{C} - \text{mol}} \cdot E \quad (2)$$

where  $E$  is number of electrons transferred to oxygen during combustion (Patel and Erickson, 1981; Battley, 1998, 1992).  $E$  can be calculated from the empirical formula of live matter

$$E = 4n_C + n_H - 2n_O - 0n_N + 5n_P + 6n_S \quad (3)$$

where  $n_C$ ,  $n_H$ ,  $n_O$ ,  $n_N$ ,  $n_P$  and  $n_S$  represent the numbers of C, H, O, N, P and S atoms in the live matter empirical formula, respectively (Patel and Erickson, 1981; Battley, 1998, 1992). Once calculated using the Patel-Erickson equation,  $\Delta_c H^\circ$  can be converted into standard enthalpy of formation,  $\Delta_f H^\circ$ , of live matter.  $\Delta_c H^\circ$  is the enthalpy change of the reaction of complete combustion of live matter.



This means that  $\Delta_c H^\circ$  can be used to find  $\Delta_f H^\circ$  of live matter using the equation (Popovic, 2022b; 2022c; 2022f; Atkins and de Paula, 2011, 2014).

$$\Delta_f H^\circ(\text{bio}) = n_C \Delta_f H^\circ(\text{CO}_2) + \frac{n_H}{2} \Delta_f H^\circ(\text{H}_2\text{O}) + \frac{n_P}{4} \Delta_f H^\circ(\text{P}_4\text{O}_{10}) + n_S \Delta_f H^\circ(\text{SO}_3) - \Delta_c H^\circ \quad (5)$$

The Battley equation gives standard molar entropy of live matter,  $S_m^\circ$ , based on its empirical formula

$$S_m^\circ(\text{bio}) = 0.187 \sum_J \frac{S_m^\circ(J)}{a_J} n_J \quad (6)$$

where  $n_J$  is the number of atoms of element  $J$  in the empirical formula of live matter (Battley, 1999; Battley and Stone, 2000).  $S_m^\circ$  and  $a_J$  are standard molar entropy and number of atoms per formula unit of element  $J$  in its standard state elemental form (Battley, 1999; Battley and Stone, 2000). The Battley equation can be modified to give standard

entropy of formation,  $\Delta_f S^\circ$ , of live matter (Battley, 1999; Battley and Stone, 2000).

$$\Delta_f S^\circ(\text{bio}) = -0.813 \sum_J \frac{S_m^\circ(J)}{a_J} n_J \quad (7)$$

Finally,  $\Delta_f H^\circ$  and  $\Delta_f S^\circ$  are combined to give standard Gibbs energy of formation of live matter,  $\Delta_f G^\circ$ .

$$\Delta_f G^\circ(\text{bio}) = \Delta_f H^\circ(\text{bio}) - T \Delta_f S^\circ(\text{bio}) \quad (8)$$

Once live matter is characterized by finding its  $\Delta_f H^\circ$ ,  $S_m^\circ$  and  $\Delta_f G^\circ$ , these properties can be combined with biosynthesis reactions to find standard thermodynamic properties of biosynthesis. Standard thermodynamic properties of biosynthesis include standard enthalpy of biosynthesis,  $\Delta_{bs} H^\circ$ , standard entropy of biosynthesis,  $\Delta_{bs} S^\circ$ , and standard Gibbs energy of biosynthesis,  $\Delta_{bs} G^\circ$ . These properties are found by applying the Hess's law to biosynthesis reactions

$$\Delta_{bs} H^\circ = \sum_{\text{products}} \nu \Delta_f H^\circ - \sum_{\text{reactants}} \nu \Delta_f H^\circ \quad (9)$$

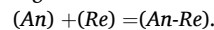
$$\Delta_{bs} S^\circ = \sum_{\text{products}} \nu S_m^\circ - \sum_{\text{reactants}} \nu S_m^\circ \quad (10)$$

$$\Delta_{bs} G^\circ = \sum_{\text{products}} \nu \Delta_f G^\circ - \sum_{\text{reactants}} \nu \Delta_f G^\circ \quad (11)$$

where  $\nu$  represents a stoichiometric coefficient (Popovic, 2022b; 2022c; 2022f; Atkins and de Paula, 2011, 2014; von Stockar, 2013a, 2013b; Battley, 1998). The most important of these three properties is standard Gibbs energy of biosynthesis, which represents the thermodynamic driving force for (von Stockar, 2013a, 2013b; von Stockar and Liu, 1999), including viruses (Popovic, 2022b; 2022c; 2022f; 2022i).

### 2.4. Thermodynamic properties of antigen-receptor binding

In order to multiply inside the cytoplasm, a virus must first enter its host cell. The first step in this process is binding of the virus antigen to the host cell receptor. The antigen of SARS-CoV-2 is the spike glycoprotein trimer (SGP) (Duan et al., 2020), while the host cell receptor is angiotensin-converting enzyme 2 (ACE2) (Scialo et al., 2020). The process of antigen-receptor binding is, in its essence, a chemical reaction, similar to protein-ligand interactions (Du et al., 2016; Popovic and Popovic, 2022). Thus, the binding of SGP to ACE2 can be described through the chemical reaction.



where (An) represents the virus antigen (SGP in the case of SARS-CoV-2), (Re) represents the host cell receptor (ACE2 for SARS-CoV-2), while (An-Re) represents the antigen-receptor complex (Du et al., 2016; Popovic and Popovic, 2022).

Like for all other chemical reactions, laws of chemical thermodynamics apply and the process of antigen-receptor binding can be described through several thermodynamic parameters. The dissociation equilibrium constant,  $K_d$ , is defined as

$$K_d = \frac{[\text{An}][\text{Re}]}{[\text{An-Re}]} \quad (12)$$

where [An] is the concentration of the virus antigen, [Re] the concentration of the host receptor and [An-Re] the concentration of the antigen-receptor complex (Du et al., 2016; Popovic and Popovic, 2022). The reciprocal of  $K_d$  is the binding equilibrium constant,  $K_B$ , (Du et al., 2016; Popovic and Popovic, 2022).

$$K_B = \frac{1}{K_d} \quad (13)$$

The binding equilibrium constant can be used to find standard Gibbs energy of binding,  $\Delta_B G^\circ$ , through the equation

$$\Delta_B G^0 = -RT \ln K_B \quad (14)$$

Where  $T$  is temperature and  $R$  is the universal gas constant (Du et al., 2016; Popovic and Popovic, 2022).

### 3. Results

Based on dissociation equilibrium constants,  $K_d$ , reported in the literature (Yue et al., 2023), standard thermodynamic properties of binding were calculated. These include the binding equilibrium constant,  $K_B$ , and standard Gibbs energy of binding,  $\Delta_B G^0$ , and are reported in Table 1. For the BQ.1.1 variant, the binding equilibrium constant is  $1.23 \times 10^8 \text{ M}^{-1}$ , and standard Gibbs energy of binding is  $-46.18 \text{ kJ/mol}$ . For the XBB/XBB.1 variant, the binding equilibrium constant is  $5.26 \times 10^7 \text{ M}^{-1}$ , and standard Gibbs energy of binding is  $-44.07 \text{ kJ/mol}$ . For the XBB.1.5 variant, the binding equilibrium constant is  $2.94 \times 10^8 \text{ M}^{-1}$ , and standard Gibbs energy of binding is  $-48.34 \text{ kJ/mol}$ . For the BA.2.75 variant, the binding equilibrium constant is  $5.56 \times 10^8 \text{ M}^{-1}$ , and standard Gibbs energy of binding is  $-49.91 \text{ kJ/mol}$ .

Based on the genetic and protein sequences reported in the literature [REF], elemental composition of nucleocapsids of the XBB.1.5 variant isolates from 5 countries were calculated for the first time, using the atom counting method (Popovic, 2022j). They are reported in form of empirical formulas in Table 2. The empirical formula of the nucleocapsid of the XBB.1.5 isolate from Chile is  $\text{CH}_{1.573540}\text{O}_{0.342703}\text{N}_{0.312374}\text{P}_{0.00603}\text{S}_{0.00336}$ . The molar mass of the empirical formula is  $23.7495 \text{ g/C-mol}$ , while the molar mass of the nucleocapsid is  $117.22 \text{ MDa}$ . The empirical formula of the nucleocapsid of the XBB.1.5 isolate from India is  $\text{CH}_{1.573611}\text{O}_{0.342616}\text{N}_{0.312358}\text{P}_{0.00601}\text{S}_{0.00336}$ . The molar mass of the empirical formula is  $23.7474 \text{ g/C-mol}$ , while the molar mass of the nucleocapsid is  $117.18 \text{ MDa}$ . The empirical formula of the nucleocapsid of the XBB.1.5 isolate from Netherlands is  $\text{CH}_{1.573562}\text{O}_{0.342674}\text{N}_{0.312371}\text{P}_{0.00602}\text{S}_{0.00336}$ . The molar mass of the empirical formula is  $23.7488 \text{ g/C-mol}$ , while the molar mass of the nucleocapsid is  $117.21 \text{ MDa}$ . The empirical formula of the nucleocapsid of the XBB.1.5 isolate from Scotland is  $\text{CH}_{1.573562}\text{O}_{0.342673}\text{N}_{0.312371}\text{P}_{0.00602}\text{S}_{0.00336}$ . The molar mass of the empirical formula is  $23.7488 \text{ g/C-mol}$ , while the molar mass of the nucleocapsid is  $117.21 \text{ MDa}$ . The empirical formula of the nucleocapsid of the XBB.1.5 isolate from USA is  $\text{CH}_{1.573529}\text{O}_{0.342714}\text{N}_{0.312379}\text{P}_{0.00603}\text{S}_{0.00336}$ . The molar mass of the empirical formula is  $23.7499 \text{ g/C-mol}$ , while the molar mass of the nucleocapsid is  $117.22 \text{ MDa}$ . These formulas were used to construct biosynthesis reactions, which are given in Table 3.

Table 4 gives standard thermodynamic properties of live matter of nucleocapsid of the XBB.1.5 variant of SARS-CoV-2. Starting from elemental composition data in Table 2, predictive biothermodynamic models (Patel-Erickson and Battley) were used to find standard thermodynamic properties of live matter for the nucleocapsid of XBB.1.5 variant. They are given in Table 5 and include standard enthalpy of formation,  $\Delta_f H^0$ , standard molar entropy,  $S_m^0$ , and standard Gibbs energy of formation,  $\Delta_f G^0$ . For the nucleocapsid of the XBB.1.5 isolate from Chile, standard enthalpy of formation is  $-75.40 \text{ kJ/C-mol}$ , standard

**Table 1**

Standard Gibbs energies of binding of SARS-CoV-2 variants. This table gives data on dissociation equilibrium constants,  $K_d$ , binding equilibrium constants,  $K_B$ , and standard Gibbs energies of binding,  $\Delta_B G^0$ , of SARS-CoV-2 variants. The analyzed SARS-CoV-2 variants are: BQ.1.1, XBB/XBB.1, XBB.1.5 and BA.2.75. All the data are at  $25^\circ\text{C}$ . The  $K_d$  data were taken from Yue et al. (2023).

Name	$K_d$ (M)	$K_B$ ( $\text{M}^{-1}$ )	$\Delta_B G^0$ (kJ/mol)
BQ.1.1	8.10E-09	1.23E+ 08	-46.18
XBB/XBB.1	1.90E-08	5.26E+ 07	-44.07
XBB.1.5	3.40E-09	2.94E+ 08	-48.34
BA.2.75	1.80E-09	5.56E+ 08	-49.91

molar entropy is  $32.49 \text{ J/C-mol K}$ , and standard Gibbs energy of formation is  $-33.28 \text{ kJ/C-mol}$ . For the nucleocapsid of the XBB.1.5 isolate from India, standard enthalpy of formation is  $-75.38 \text{ kJ/C-mol}$ , standard molar entropy is  $32.49 \text{ J/C-mol K}$ , and standard Gibbs energy of formation is  $-33.26 \text{ kJ/C-mol}$ . For the nucleocapsid of the XBB.1.5 isolate from Netherlands, standard enthalpy of formation is  $-75.39 \text{ kJ/C-mol}$ , standard molar entropy is  $32.49 \text{ J/C-mol K}$ , and standard Gibbs energy of formation is  $-33.27 \text{ kJ/C-mol}$ . For the nucleocapsid of the XBB.1.5 isolate from Scotland, standard enthalpy of formation is  $-75.39 \text{ kJ/C-mol}$ , standard molar entropy is  $32.49 \text{ J/C-mol K}$ , and standard Gibbs energy of formation is  $-33.27 \text{ kJ/C-mol}$ . For the nucleocapsid of the XBB.1.5 isolate from USA, standard enthalpy of formation is  $-75.40 \text{ kJ/C-mol}$ , standard molar entropy is  $32.49 \text{ J/C-mol K}$ , and standard Gibbs energy of formation is  $-33.28 \text{ kJ/C-mol}$ .

Table 5 gives standard thermodynamic properties of biosynthesis of the nucleocapsid of the XBB.1.5 variant of SARS-CoV-2. Biosynthesis stoichiometry data from Table 3 were combined with standard thermodynamic properties of live matter from Table 4, to find for the first time standard thermodynamic properties of biosynthesis. These are presented in Table 5 and include standard enthalpy of biosynthesis,  $\Delta_{bs} H^0$ , standard entropy of biosynthesis,  $\Delta_{bs} S^0$ , and standard Gibbs energy of biosynthesis,  $\Delta_{bs} G^0$ . For the nucleocapsid of the XBB.1.5 isolate from Chile, standard enthalpy of biosynthesis is  $-232.33 \text{ kJ/C-mol}$ , standard entropy of biosynthesis is  $-37.34 \text{ J/C-mol K}$ , and standard Gibbs energy of biosynthesis is  $-221.23 \text{ kJ/C-mol}$ . For the nucleocapsid of the XBB.1.5 isolate from India, standard enthalpy of biosynthesis is  $-232.27 \text{ kJ/C-mol}$ , standard entropy of biosynthesis is  $-37.33 \text{ J/C-mol K}$ , and standard Gibbs energy of biosynthesis is  $-221.18 \text{ kJ/C-mol}$ . For the nucleocapsid of the XBB.1.5 isolate from Netherlands, standard enthalpy of biosynthesis is  $-232.32 \text{ kJ/C-mol}$ , standard entropy of biosynthesis is  $-37.34 \text{ J/C-mol K}$ , and standard Gibbs energy of biosynthesis is  $-221.22 \text{ kJ/C-mol}$ . For the nucleocapsid of the XBB.1.5 isolate from Scotland, standard enthalpy of biosynthesis is  $-232.32 \text{ kJ/C-mol}$ , standard entropy of biosynthesis is  $-37.34 \text{ J/C-mol K}$ , and standard Gibbs energy of biosynthesis is  $-221.22 \text{ kJ/C-mol}$ . For the nucleocapsid of the XBB.1.5 isolate from USA, standard enthalpy of biosynthesis is  $-232.34 \text{ kJ/C-mol}$ , standard entropy of biosynthesis is  $-37.34 \text{ J/C-mol K}$ , and standard Gibbs energy of biosynthesis is  $-221.25 \text{ kJ/C-mol}$ .

### 4. Discussion

The Omicron XBB.1.5 variant represents the latest step in the evolution of SARS-CoV-2. It is characterized by a specific empirical formula, different from those of all other SARS-CoV-2 variants. The difference in empirical formulas originates from new mutations, which make it different from other variants. The differences in empirical formulas lead to differences in thermodynamic properties of formation and biosynthesis. Moreover, mutations in the RNA segment encoding the spike glycoprotein cause changes in binding affinity, thermodynamic properties of binding and clinical properties – infectivity. Furthermore, they lead to changes in kinetic properties – binding rate and multiplication rate of the virus (Popovic, 2022ji).

The Omicron XBB.1.5 variant is in co-circulation with other variants, present in various countries throughout the world. The XBB.1.5 variant competes with other variants. In the public, a question is raised of whether the XBB.1.5 variant will be able to outcompete the other variants, suppress them and cause another pandemic wave (WHO, 2023). Competition of viruses and virus variants has been described in the literature (Popovic and Minceva, 2021a). Through the procedure described in the methodology section, using the atom counting method, the empirical formula of the XBB.1.5 variant was calculated. Table 2 gives empirical formulas of different isolates of the XBB.1.5 variant taken from different components. The results given in Table 2 show that isolates taken from the same continent exhibit similarity. On the other hand, isolates taken from different continents exhibit greater

**Table 2**

Empirical formulas of the nucleocapsid of XBB.1.5 variant of SARS-CoV-2. This table gives elemental composition in form of empirical formulas. The general empirical formula has the form  $C_nH_mO_nN_nP_nS_n$ . The table gives data for XBB.1.5 isolates from 5 countries. In addition, molar masses were reported for the empirical formulas,  $Mr$ , and for entire nucleocapsids,  $Mr(nc)$ .

Name	C	H	O	N	P	S	Mr (g/C-mol)	Mr (nc) (MDa)
XBB.1.5 - Chile	1	1.573540	0.342703	0.312374	0.00603	0.00336	23.7495	117.22
XBB.1.5 - India	1	1.573611	0.342616	0.312358	0.00601	0.00336	23.7474	117.18
XBB.1.5 - Netherlands	1	1.573562	0.342674	0.312371	0.00602	0.00336	23.7488	117.21
XBB.1.5 - Scotland	1	1.573562	0.342673	0.312371	0.00602	0.00336	23.7488	117.21
XBB.1.5 - USA	1	1.573529	0.342714	0.312379	0.00603	0.00336	23.7499	117.22

**Table 3**

Biosynthesis stoichiometry of the nucleocapsid XBB.1.5 variant of SARS-CoV-2. The general biosynthesis reaction has the form: (Amino acids) +  $O_2$  +  $HPO_4^{2-}$  +  $HCO_3^-$  → (Bio) +  $SO_4^{2-}$  +  $H_2O$  +  $H_2CO_3$ , where (Bio) denotes the empirical formula of live matter from Table 1. The stoichiometric coefficients for the biosynthesis reactions are given in this table.

Name	Reactants				→	Products			
	Amino acid	$O_2$	$HPO_4^{2-}$	$HCO_3^-$		Bio	$SO_4^{2-}$	$H_2O$	$H_2CO_3$
XBB.1.5 - Chile	1.3901	0.4913	0.0060	0.0437	→	1	0.0279	0.0538	0.4338
XBB.1.5 - India	1.3900	0.4911	0.0060	0.0437	→	1	0.0279	0.0538	0.4337
XBB.1.5 - Netherlands	1.3901	0.4912	0.0060	0.0437	→	1	0.0279	0.0538	0.4338
XBB.1.5 - Scotland	1.3901	0.4912	0.0060	0.0437	→	1	0.0279	0.0538	0.4338
XBB.1.5 - USA	1.3901	0.4913	0.0060	0.0437	→	1	0.0279	0.0538	0.4338

**Table 4**

Standard thermodynamic properties of live matter for the nucleocapsid of XBB.1.5 variant of SARS-CoV-2. This table gives data on standard enthalpies of formation,  $\Delta_f H^\circ$ , standard molar entropies,  $S_m^\circ$ , and standard Gibbs energies of formation,  $\Delta_f G^\circ$ .

Name	$\Delta_f H^\circ$ (kJ/C-mol)	$S_m^\circ$ (J/C-mol K)	$\Delta_f G^\circ$ (kJ/C-mol)
XBB.1.5 - Chile	-75.40	32.49	-33.28
XBB.1.5 - India	-75.38	32.49	-33.26
XBB.1.5 - Netherlands	-75.39	32.49	-33.27
XBB.1.5 - Scotland	-75.39	32.49	-33.27
XBB.1.5 - USA	-75.40	32.49	-33.28

**Table 5**

Standard thermodynamic properties of biosynthesis of the nucleocapsid of the XBB.1.5 variant of SARS-CoV-2. This table gives data on standard enthalpies of biosynthesis,  $\Delta_{bs} H^\circ$ , standard entropies of biosynthesis,  $\Delta_{bs} S^\circ$ , and standard Gibbs energies of biosynthesis,  $\Delta_{bs} G^\circ$ .

Name	$\Delta_{bs} H^\circ$ (kJ/C-mol)	$\Delta_{bs} S^\circ$ (J/C-mol K)	$\Delta_{bs} G^\circ$ (kJ/C-mol)
XBB.1.5 - Chile	-232.33	-37.34	-221.23
XBB.1.5 - India	-232.27	-37.33	-221.18
XBB.1.5 - Netherlands	-232.32	-37.34	-221.22
XBB.1.5 - Scotland	-232.32	-37.34	-221.22
XBB.1.5 - USA	-232.34	-37.34	-221.25

differences. Since differences appear as a consequence of replacement of nucleotides that appear due to mutations, we can conclude that the XBB.1.5 variant also exhibits a tendency to mutate and that in the future new variants are likely to appear.

Based on the empirical formula and biosynthesis reactions, Gibbs energy of biosynthesis of the XBB.1.5 isolates was calculated. Gibbs energy of biosynthesis indicates the multiplication rate, since it represents the driving force for virus multiplication (Popovic, 2022f; 2022i). More negative Gibbs energy of biosynthesis indicates a greater rate of reactions of replication, transcription and translation. A greater rate of virus multiplication leads to greater damage of host cells and greater excretion of newly synthesized virions into the environment, which influences the inoculation dose. The inoculation dose is expressed through the number of virions per  $cm^3$  of air. Infectivity is also influenced by Gibbs energy of antigen-receptor binding. The mutated receptor of the

XBB.1.5 variant has led to changes in affinity (dissociation constant). Changes in dissociation constant lead to changes in Gibbs energy of binding, according to the binding phenomenological equation (Popovic and Popovic, 2022; Popovic, 2022b; 2022g). The increased rate of binding leads to increased infectivity. Standard Gibbs energy of binding of the XBB.1.5 variant is  $-48.34$  kJ/mol. Standard Gibbs energies of binding of the other variants are:  $-46.18$  kJ/mol for BQ.1.1,  $-44.07$  kJ/mol for XBB/XBB.1, and  $-49.91$  kJ/mol for BA.2.75. Thus, XBB.1.5 has a standard Gibbs energy of binding more negative than those of the BQ.1.1 and XBB/XBB.1 variants, but less negative than that of the BA.2.75 variant. This leads to the conclusion that the rate of antigen-receptor binding of the XBB.1.5 variant will be lower than that of the Omicron BA.2.75 variant. In that case, the infectivity of XBB.1.5 should be lower. Thus, even though there are reasons for being careful, it seems that the thermodynamic driving force of binding does not indicate a greater danger in terms of infectivity than for the case of BA.2.75 variant. However, infectivity depends on the concentration of virus particles in the air and excretion. These depend on the virus multiplication rate. The virus multiplication rate depends on Gibbs energy of biosynthesis, since it represents the driving force for multiplication. Gibbs energy of biosynthesis for that variant is very similar to the other Omicron variants:  $-221.18$  kJ/C-mol for BQ.1.1 (Popovic, 2022h),  $-221.25$  kJ/C-mol for XBB (Popovic, 2022h),  $-221.19$  for XBB.1 (Popovic, 2022h), and  $-221.18$  kJ/C-mol for BA.2.75 (Popovic, 2022f). Thus, Gibbs energy of biosynthesis deviates very little for various variants of SARS-CoV-2. This implies that the rate of multiplication of the XBB.1.5 variant will be very similar to the multiplication rate of the other variants. The degree of damage to cells and tissues, as well as virus excretion, will be similar for all the Omicron variants. This implies that the mutations that appeared in the Omicron variants have influenced more the antigen-receptor binding rate, than the virus multiplication rate.

## 5. Conclusions

The XBB.1.5 isolates from Europe (Scotland and Netherlands) exhibit the greatest similarity in elemental composition and thermodynamic properties. This indicates the very similar mutations in the two European isolates. However, the isolates from other continents - South America (Chile), Asia (India) and North America (USA) exhibit differences in elemental composition and thermodynamic properties. It seems

that the XBB.1.5 variant exhibits further tendency towards mutation.

Gibbs energies of biosynthesis of the XBB.1.5 variant is similar to those of other Omicron variants. Thus, we can expect the pathogenicity of these variants to be equal.

Gibbs energy of binding of the XBB.1.5 variant is more negative than those of most of the other Omicron variants (BQ.1.1 and XBB/XBB.1). However, it is not more negative than that of the BA.2.75. Thus, we can expect the infectivity of the XBB.1.5 should be lower than that of the BA.2.75.

### CRedit authorship contribution statement

**Marko Popovic:** Conceptualization, Methodology, Software, Validation, Formal analysis, Investigation, Writing – original draft, Writing – review & editing.

### Data Availability

The used data are described in the methods section.

### Acknowledgements

The author gratefully acknowledges all data contributors, i.e., the Authors and their Originating laboratories responsible for obtaining the specimens, and their Submitting laboratories for generating the genetic sequence and metadata and sharing via the GISAID Initiative, on which this research is based.

### References

- Atkins, P.W., de Paula, J., 2011. *Physical Chemistry for the Life Sciences* (2nd edition), W. H. Freeman and Company. ISBN-13: 978-1429231145.
- Atkins, P.W., de Paula, J., 2014. *Physical Chemistry: Thermodynamics, Structure, and Change*, 10th Edition. New York: W. H. Freeman and Company. ISBN-13: 978-1429290197.
- Balmer, R.T., 2010. *Modern Engineering Thermodynamics*. Academic Press, Cambridge, MA. <https://doi.org/10.1016/C2009-0-20199-1>.
- Battley, E.H., 1992. On the enthalpy of formation of *Escherichia coli* K-12 cells. *Biotechnol. Bioeng.* 39, 5–12. <https://doi.org/10.1002/bit.260390103>.
- Battley, E.H., 1998. The development of direct and indirect methods for the study of the thermodynamics of microbial growth. *Thermochim. Acta* 309 (1–2), 17–37. [https://doi.org/10.1016/S0040-6031\(97\)00357-2](https://doi.org/10.1016/S0040-6031(97)00357-2).
- Battley, E.H., 1999. An empirical method for estimating the entropy of formation and the absolute entropy of dried microbial biomass for use in studies on the thermodynamics of microbial growth. *Thermochim. Acta* 326 (1–2), 7–15. [https://doi.org/10.1016/S0040-6031\(98\)00584-X](https://doi.org/10.1016/S0040-6031(98)00584-X).
- Battley, E.H., Stone, J.R., 2000. A comparison of values for the entropy and the entropy of formation of selected organic substances of biological importance in the solid state, as determined experimentally or calculated empirically. *Thermochim. Acta* 349 (1–2), 153–161. [https://doi.org/10.1016/S0040-6031\(99\)00509-2](https://doi.org/10.1016/S0040-6031(99)00509-2).
- Browne, E., 2023. Why COVID's XBB.1.5 'Kraken' Variant Is So Contagious. [Online] *Scientific American*. Available at: <https://www.scientificamerican.com/article/why-covids-xbb-1-5-kraken-variant-is-so-contagious/> (Accessed on January 10, 2023).
- Degueldre, C., 2021. Single virus inductively coupled plasma mass spectroscopy analysis: A comprehensive study. *Talanta* 228, 122211. <https://doi.org/10.1016/j.talanta.2021.122211>.
- Demirel, Y., 2014. *Nonequilibrium Thermodynamics: Transport and Rate Processes in Physical, Chemical and Biological Systems*, 3rd ed. Amsterdam: Elsevier. ISBN: 9780444595812.
- Du, X., Li, Y., Xia, Y.L., Ai, S.M., Liang, J., Sang, P., Liu, S.Q., 2016. Insights into protein-ligand interactions: mechanisms, models, and methods. *Int. J. Mol. Sci.* 17 (2), 144. <https://doi.org/10.3390/ijms17020144>.
- Duan, L., Zheng, Q., Zhang, H., Niu, Y., Lou, Y., Wang, H., 2020. The SARS-CoV-2 spike glycoprotein biosynthesis, structure, function, and antigenicity: implications for the design of spike-based vaccine immunogens. *Front. Immunol.* 11, 576622. <https://doi.org/10.3389/fimmu.2020.576622>.
- Elbe, S., Buckland-Merrett, G., 2017. Data, disease and diplomacy: GISAID's innovative contribution to global health. *Glob. Chall.* 1, 33–46. <https://doi.org/10.1002/gch2.1018>.
- Gale, P., 2018. Using thermodynamic parameters to calibrate a mechanistic dose-response for infection of a host by a virus. *Microb. Risk Anal.* 8, 1–13. <https://doi.org/10.1016/j.mran.2018.01.002>.
- Gale, P., 2019. Towards a thermodynamic mechanistic model for the effect of temperature on arthropod vector competence for transmission of arboviruses. *Microb. Risk Anal.* 12, 27–43. <https://doi.org/10.1016/j.mran.2019.03.001>.
- Gale, P., 2020. How virus size and attachment parameters affect the temperature sensitivity of virus binding to host cells: predictions of a thermodynamic model for arboviruses and HIV. *Microb. Risk Anal.* 15, 100104. <https://doi.org/10.1016/j.mran.2020.100104>.
- Gale, P., 2022. Using thermodynamic equilibrium models to predict the effect of antiviral agents on infectivity: Theoretical application to SARS-CoV-2 and other viruses. *Microb. Risk Anal.* 21, 100198. <https://doi.org/10.1016/j.mran.2021.100198>.
- GISAID, 2023. GISAID database. [Online] Available at: <https://gisaid.org/> (Accessed on January 17, 2023).
- Gullar, M.P., Meiriño, R., Donat-Vargas, C., Corral, O., Jouvé, N., Soriano, V., 2020. Inoculum at the time of SARS-CoV-2 exposure and risk of disease severity. *Int. J. Infect. Dis.: IJID: Off. Publ. Int. Soc. Infect. Dis.* 97, 290–292. <https://doi.org/10.1016/j.ijid.2020.06.035>.
- Head, R.J., Lumbers, E.R., Jarrott, B., Tretter, F., Smith, G., Pringle, K.G., Islam, S., Martin, J.H., 2022. Systems analysis shows that thermodynamic physiological and pharmacological fundamentals drive COVID-19 and response to treatment. *Pharmacol. Res. Perspect.* 10 (1), e00922. <https://doi.org/10.1002/prp2.922>.
- Kaniadakis, G., Baldi, M.M., Deisboeck, T.S., Grisolia, G., Hristopoulos, D.T., Scarfone, A. M., Sparavigna, A., Wada, T., Lucia, U., 2020. The  $\kappa$ -statistics approach to epidemiology. *Sci. Rep.* 10 (1), 19949. <https://doi.org/10.1038/s41598-020-76673-3>.
- Khare, S., et al., 2021. GISAID's role in pandemic response. *China CDC Wkly.* 3 (49), 1049–1051. <https://doi.org/10.46234/ccdcw2021.255>.
- Lucia, U., Grisolia, G., Deisboeck, T.S., 2020a. Seebeck-like effect in SARS-CoV-2 biothermodynamics. *Atti della Accademia Peloritana dei Pericolanti-Classe di Scienze Fisiche. Mat. e Nat.* 98 (2), 6. <https://doi.org/10.1478/AAPP.982A6>.
- Lucia, U., Deisboeck, T.S., Grisolia, G., 2020b. Entropy-based pandemics forecasting. *Front. Phys.* 8, 274. <https://doi.org/10.3389/fphy.2020.00274>.
- Lucia, U., Grisolia, G., Deisboeck, T.S., 2021. Thermodynamics and SARS-CoV-2: neurological effects in post-Covid 19 syndrome. *Atti della Accad. Peloritana dei Pericolanti* 99 (2), A3. <https://doi.org/10.1478/AAPP.992A3>.
- Nadi, F., Özligen, M., 2021. Effects of COVID-19 on energy savings and emission reduction: a case study. *Int. J. Glob. Warm.* 25 (1), 38–57. <https://doi.org/10.1504/IJGW.2021.117432>.
- National Center for Biotechnology Information, 2022. NCBI Database [online]. Available at: <https://www.ncbi.nlm.nih.gov/> (Accessed on January 7, 2023).
- Neuman, B.W., Buchmeier, M.J., 2016. Supramolecular architecture of the coronavirus particle. *Adv. Virus Res.* 96, 1–27. <https://doi.org/10.1016/bs.aivir.2016.08.005>.
- Neuman, B.W., Adair, B.D., Yoshioka, C., Quispe, J.D., Orca, G., Kuhn, P., Milligan, R.A., Yeager, M., Buchmeier, M.J., 2006. Supramolecular architecture of severe acute respiratory syndrome coronavirus revealed by electron cryomicroscopy. *J. Virol.* 80 (16), 7918–7928. <https://doi.org/10.1128/JVI.00645-06>.
- Neuman, B.W., Kiss, G., Kunding, A.H., Bhella, D., Baksh, M.F., Connelly, S., Droese, B., Klaus, J.P., Makino, S., Sawicki, S.G., Siddell, S.G., Stamo, D.G., Wilson, I.A., Kuhn, P., Buchmeier, M.J., 2011. A structural analysis of M protein in coronavirus assembly and morphology. *J. Struct. Biol.* 174 (1), 11–22. <https://doi.org/10.1016/j.jsb.2010.11.021>.
- Özligen, M., Yilmaz, B., 2021. COVID-19 disease causes an energy supply deficit in a patient. *Int. J. Energy Res.* 45 (2), 1157–1160. <https://doi.org/10.1002/er.5883>.
- Patel, S.A., Erickson, L.E., 1981. Estimation of heats of combustion of biomass from elemental analysis using available electron concepts. *Biotechnol. Bioeng.* 23, 2051–2067. <https://doi.org/10.1002/bit.260230910>.
- Phan, T., 2020. Genetic diversity and evolution of SARS-CoV-2. *Infect. Genet. Evol.* 81, 104260. <https://doi.org/10.1016/j.meegid.2020.104260>.
- Popovic, M., 2022f. Omicron BA.2.75 Sublineage (Centaurus) Follows the Expectations of the Evolution Theory: Less Negative Gibbs Energy of Biosynthesis Indicates Decreased Pathogenicity. *Microbiology Research*, 13(4), 937–952. MDPI AG. Retrieved from <https://doi.org/10.3390/microbiolres13040066>.
- Popovic, M., 2022g. Omicron BA.2.75 Subvariant of SARS-CoV-2 Is Expected to Have the Greatest Infectivity Compared with the Competing BA.2 and BA.5, Due to Most Negative Gibbs Energy of Binding. *BioTechnol.* 11(4), 45. MDPI AG. Retrieved from <https://doi.org/10.3390/biotech11040045>.
- Popovic, M., 2022a. Strain wars 2: binding constants, enthalpies, entropies, Gibbs energies and rates of binding of SARS-CoV-2 variants. *Virology* 570, 35–44. <https://doi.org/10.1016/j.virol.2022.03.008>.
- Popovic, M., 2022b. Strain wars 3: differences in infectivity and pathogenicity between Delta and Omicron strains of SARS-CoV-2 can be explained by thermodynamic and kinetic parameters of binding and growth. *Microb. Risk Anal.* 22, 100217. <https://doi.org/10.1016/j.mran.2022.100217>.
- Popovic, M., 2022c. Strain wars 4 - Darwinian evolution through Gibbs' glasses: Gibbs energies of binding and growth explain evolution of SARS-CoV-2 from Hu-1 to BA.2. *Virology* 575, 36–42. <https://doi.org/10.1016/j.virol.2022.08.009>.
- Popovic, M., 2022d. Strain wars 5: Gibbs energies of binding of BA.1 through BA.4 variants of SARS-CoV-2. *Microb. Risk Anal.* 22, 100231. <https://doi.org/10.1016/j.mran.2022.100231>.
- Popovic, M., 2022e. Beyond COVID-19: Do biothermodynamic properties allow predicting the future evolution of SARS-CoV-2 variants. *Microb. Risk Anal.* 22, 100232. <https://doi.org/10.1016/j.mran.2022.100232>.
- Popovic, M., 2022h. Never Ending Story? Biothermodynamic Properties of Biosynthesis and Binding of Omicron BQ.1, BQ.1.1, XBB and XBB.1 variants of SARS-CoV-2. *Preprints* 2022120122. <https://doi.org/10.20944/preprints202212.0122.v1>.
- Popovic, M., 2022i. Biothermodynamics of viruses from absolute zero (1950) to virothermodynamics (2022). *Vaccines* 10 (12), 2112. <https://doi.org/10.3390/vaccines10122112>.
- Popovic, M., 2022j. Atom counting method for determining elemental composition of viruses and its applications in biothermodynamics and environmental science. *Comput. Biol. Chem.* 96, 107621. <https://doi.org/10.1016/j.compbiolchem.2022.107621>.

- Popovic, M., Minceva, M., 2021a. Coinfection and interference phenomena are the results of multiple thermodynamic competitive interactions. *Microorganisms* 9 (10), 2060. <https://doi.org/10.3390/microorganisms9102060>.
- Popovic, M., Popovic, M., 2022. Strain wars: competitive interactions between SARS-CoV-2 strains are explained by Gibbs energy of antigen-receptor binding. *Microb. Risk Anal.* 21, 100202. <https://doi.org/10.1016/j.mran.2022.100202>.
- Sayers, E.W., Bolton, E.E., Brister, J.R., Canese, K., Chan, J., Comeau, D.C., Connor, R., Funk, K., Kelly, C., Kim, S., Madej, T., Marchler-Bauer, A., Lanczycki, C., Lathrop, S., Lu, Z., Thibaud-Nissen, F., Murphy, T., Phan, L., Skripchenko, Y., Tse, T., Sherry, S. T., 2022. Database resources of the national center for biotechnology information. *Nucleic Acids Res.* 50 (D1), D20–D26. <https://doi.org/10.1093/nar/gkab1112>.
- Scialo, F., Daniele, A., Amato, F., Pastore, L., Matera, M.G., Cazzola, M., Castaldo, G., Bianco, A., 2020. ACE2: the major cell entry receptor for SARS-CoV-2. *Lung* 198 (6), 867–877. <https://doi.org/10.1007/s00408-020-00408-4>.
- Shu, Y., McCauley, J., 2017. GISAID: from vision to reality. *EuroSurveillance*, 22(13) doi: 10.2807/1560-7917.ES.2017.22.13.30494 PMID: PMC5388101.
- Şimşek, B., Özilgen, M., Utku, F.Ş., 2021. How much energy is stored in SARS-CoV-2 and its structural elements? *Energy Storage*, e298. <https://doi.org/10.1002/est2.298>.
- Singh, D., Yi, S.V., 2021. On the origin and evolution of SARS-CoV-2. *Exp. Mol. Med.* 53 (4), 537–547. <https://doi.org/10.1038/s12276-021-00604-z>.
- Spinelli, M.A., Glidden, D.V., Gennatas, E.D., Bielecki, M., Beyrer, C., Rutherford, G., Chambers, H., Goosby, E., Gandhi, M., 2021. Importance of non-pharmaceutical interventions in lowering the viral inoculum to reduce susceptibility to infection by SARS-CoV-2 and potentially disease severity. *Lancet Infect. Dis.* 21 (9), e296–e301. [https://doi.org/10.1016/S1473-3099\(20\)30982-8](https://doi.org/10.1016/S1473-3099(20)30982-8).
- Stacy, K., 2023. COVID-19 Omicron Variant "Kraken" Is Even More Transmissible Than Ever. [Online] *The Science Times*. Available at: <https://www.sciencetimes.com/articles/41744/20230108/covid-19-omicron-variant-kraken-even-more-transmissible.htm> (Accessed on January 10, 2023).
- Tang, X., Wu, C., Li, X., Song, Y., Yao, X., Wu, X., Lu, J., 2020. On the origin and continuing evolution of SARS-CoV-2. *Natl. Sci. Rev.* 7 (6), 1012–1023. <https://doi.org/10.1093/nsr/nwaa036>.
- Van Damme, W., Dahake, R., van de Pas, R., Vanham, G., Assefa, Y., 2021. COVID-19: does the infectious inoculum dose-response relationship contribute to understanding heterogeneity in disease severity and transmission dynamics. *Med. Hypotheses* 146, 110431. <https://doi.org/10.1016/j.mehy.2020.110431>.
- von Stockar, U., Liu, J., 1999. Does microbial life always feed on negative entropy? Thermodynamic analysis of microbial growth. *Biochim. Et. Biophys. Acta* 1412 (3), 191–211. [https://doi.org/10.1016/s0005-2728\(99\)00065-1](https://doi.org/10.1016/s0005-2728(99)00065-1).
- Von Stockar, U., 2013a. Live cells as open non-equilibrium systems. In Urs von Stockar, ed., *Biothermodynamics: The Role of Thermodynamics in Biochemical Engineering*, Lausanne: EPFL Press, 475–534. <https://doi.org/10.1201/b15428>.
- Von Stockar, U., 2013b. Biothermodynamics of live cells: energy dissipation and heat generation in cellular structures. In: von Stockar, U. (Ed.), *Biothermodynamics: The Role of Thermodynamics in Biochemical Engineering*. EPFL Press, Lausanne, pp. 475–534. <https://doi.org/10.1201/b15428>.
- WHO, 2023. XBB.1.5 Rapid risk assessment, 11 January 2023. [Online] World Health Organization. Available at: [https://www.who.int/docs/default-source/coronaviruse/11jan2023\\_xbb15\\_rapid\\_risk\\_assessment.pdf](https://www.who.int/docs/default-source/coronaviruse/11jan2023_xbb15_rapid_risk_assessment.pdf) (Accessed on January 15, 2023).
- Yilmaz, B., Ercan, S., Akduman, S., Özilgen, M., 2020. Energetic and exergetic costs of COVID-19 infection on the body of a patient. *Int. J. Exergy* 32 (3), 314–327. <https://doi.org/10.1504/IJEX.2020.10030515>.
- Yue, C., Song, W., Wang, L., Jian, F., Chen, X., Gao, F., Cao, Y.R., 2023. Enhanced transmissibility of XBB. 1.5 is contributed by both strong ACE2 binding and antibody evasion. *bioRxiv*. <https://doi.org/10.1101/2023.01.03.522427>.